Journal: Canadian Geotechnical Journal

Submitted: 24/04/2023

Title: **A three-dimensional study of vegetation management on cut slopes**

Authors: Dr Aikaterini Tsiampousi

Imperial College London
Department of Civil & Environmental Engineering
London, U.K.

Corresponding Author: Dr Aikaterini Tsiampousi MEng MSc DIC PhD
Senior Lecturer
Imperial College London
Department of Civil & Environmental Engineering
Skempton Building
London SW7 2AZ
UK
Tel: +44 (0)20 7594 6020
aikaterini.tsiampousi@imperial.ac.uk

Competing interests: The authors declare there are no competing interests.

Total number of words: 7948 words, 16 figures, 2 tables (equivalent of 12,448 words)

A three-dimensional study of vegetation management on cut slopes

Tsiampousi, A.

Abstract

Infrastructure slopes often become covered in dense vegetation due to poor vegetation management. Despite increasing cohesion and enhancing slope stability, high water demand vegetation leads to serviceability problems, primarily towards the end of the summer. Drastic approaches, however, such as vegetation clearance, have caused instabilities during wet seasons. Therefore, appropriate, effective, and continuous vegetation management is of essence and should consider both biodiversity and the engineering asset, while accounting for the contribution of vegetation in battling climate change. Developing numerical methodologies and models can be particularly useful in acquiring insight into the complex mechanism and processes taking place during slope-plant-atmosphere interactions. The work presented here focused for the first time on combining three-dimensional stability and serviceability issues through the development of a 3D numerical model to investigate different vegetation management strategies for a slope covered in high evapotranspiration demand vegetation and suffering serviceability problems. Different 3D patterns of vegetation removal and of replacement with lower water demand vegetation were considered and the effect of each of these on the serviceability and stability of the slope during the subsequent year was examined. The results demonstrated that replacement was preferable to removal, as stability and serviceability should be considered concurrently, and that, occasionally, clearance may have detrimental effects not only on stability but also on serviceability. The importance of considering out-of-plane displacements, which have traditionally been ignored, was revealed, thus providing numerical evidence that a shift in field monitoring is required, to capture the three-dimensionality of the problem.

Key words: slope stability, serviceability, vegetation, precipitation, soil-atmosphere interaction, 3-dimentional effects

Introduction

Vegetation affects the geotechnical infrastructure on which it grows in multiple ways: from altering the hydraulic (e.g. Leung et al., 2015; Ni et al., 2019a; Dias et al., 2021) and mechanical properties (e.g. Yildiz et al., 2018; Fraccica et al., 2020) of the rooted zone and altering the pore water pressures and the coefficient of earth pressure at rest at depths far exceeding the depth of the rooted zone (Tsiampousi et al., 2014), to contributing with its weight to the stability or instability of sloping ground (Greenwood et al., 2004). Desiccation cracks may form under prevailing evapotranspiration during dry periods (Li & Zhang, 2011), increasing mass soil permeability and promoting water ingress during subsequent wet periods, inducing instabilities (Ng et al., 2001). Ng et al. (2022) provided a thorough review of the state of the art in relation to the hydraulic and mechanical reinforcement of the soil due to the presence of roots, highlighting among other key points, the influence of root architecture.

Significant work has been carried out in developing appropriate constitutive models which capture the mechanical and hydraulic reinforcement. Switala et al. (2019) presented a critical state type model which accounted for the root strength and its progressive activation through the increase of preconsolidation pressure (root hardening). Ng et al. (2022) introduced a constitutive model that coupled root effects with the cyclic thermo-mechanical unsaturated soil behaviour. Both models present significant advances over the customary approach of increasing cohesion and present a practical and realistic alternative to analytical models reviewed by Wu (2012). In terms of hydraulic modelling, the work of Ni et al. (2019b) highlighted the differences between bare, single- and mixed-species vegetated soil, and underlined the effect of root decay in the value of saturated permeability. Importantly, it provided means for modelling these effects on soil permeability and soil-water retention curve. Despite the significant advances in the constitutive modelling of rooted zones, a methodology has not yet been developed on how to incorporate them in numerical analyses where vegetation is either cleared or replaced by a different type, and specifically how to deal with the imposed decrease in strength. This becomes a prohibitive issue in numerical analyses where soil states lie on or very close to a certain yield surface corresponding to a certain vegetation type, and the size of the new yield surface, for the new vegetation type, leaves these soil states outside, i.e., representing an impossible stress state.

In addition to slope stability, serviceability problems have been related to the presence of vegetation, primarily when evapotranspiration is high (O'Brien, 2013). Tsiampousi et al. (2017) studied numerically the whole life cycle of a slope cut in London clay, demonstrating that high water demand vegetation enhances slope stability but at the expense of serviceability. Vegetation clearance on the other hand, may lead to a rapid loss of stability. These findings are supported by field measurements in similar cut and embankment slopes (Smethurst et al., 2012; Smethurst et al., 2015) and highlight the importance of vegetation management in preserving engineering assets.

Owing to the complexity of the coupled hydro-mechanical processes taking place, numerical analysis has proved to be a useful tool in studying soil-atmosphere interaction (Elias et al., 2017), with multiple breakthroughs, from the early attempts of incorporating winter and summer pore water pressure profiles (e.g. Russell et al., 2000; Kovacevic et al., 2001; Nyambayo et al., 2004; O'Brien et al., 2004; Lees et al., 2013), to performing non-coupled (e.g. Tsaparas et al., 2002; Rouainia et al., 2009) and fully-coupled (e.g. Tsiampousi et al., 2017; Pedone et al., 2022; Sitarenios et al., 2021) 2D hydro-mechanical numerical analyses. Switala et al. (2018) considered the effect of vegetation on resisting rainfall induced slope failure in a fully-coupled 3D analysis, demonstrating the beneficial effect of accounting for the additional strength of the vegetated soil. Mao et al. (2014) considered different vegetation scenarios in 3D and studied their effect on slope stability, employing a linear elastic perfectly plastic Mohr-Coulomb model and modifying the soil parameters to account for the effect of roots. They demonstrated that depending on the presence and density of roots beneath the superficial rooted zone, the Factor of Safety may increase by 15% and in certain cases over 25%. More recently, Ng et al. (2021) presented a comprehensive theoretical 3D model to capture hydro-mechanical effects of root systems on slope stability.

Notably, they differentiated between primary and secondary roots, introducing a pull-out force for the former and an increased cohesion term for the latter. Tsiampousi (2023a) studied the effect of vegetation removal on the stability of a cut slope in a series of fully-coupled 3D analyses, providing useful albeit preliminary insights into 3D effects. Similar to the previous works, the work by Tsiampousi (2023a) focused on slope stability with no consideration for serviceability. It should be noted that the selection of soil model – a linear elastic perfectly plastic Mohr-Coulomb model, where stiffness is independent of stress and strain level – was a major limitation that prevented the combined study of stability and serviceability.

This work builds on the work of Tsiampousi et al. (2017), which was loosely based on the case study by Smethurst et al. (2012) from a cut slope in Newbury, SE England. Rather than focusing on the whole-life cycle of the slope in 2D, as Tsiampousi et al. (2017), the current study expands on the subject of vegetation management, considering a plethora of different scenarios where high water demand vegetation is either removed entirely or replaced by vegetation of lower water demand, following various 3D geometrical patterns, in order to establish good practice with reference to both stability and serviceability. Although Lobmann et al. (2020) and Ng et al. (2021) also studied the effect of different vegetation types and/or vegetation spacing on slope stability, there are two major points of differentiation between this and previous works: (a) this work extends to serviceability, whereas previous works focused only on stability and (b) change of vegetation type and/or vegetation clearance is modelled as part of the on-going analysis, whereas in previous work different vegetation types or topology were considered in separate analyses. The second point necessitated some modelling simplifications, in that the hydro-mechanical reinforcement that the roots provide to the soil could not be easily and robustly incorporated in the analysis, as explained above. Nonetheless, ignoring the direct effect of roots facilitates significant computational savings, and provides a safe estimate of the factor of safety, as the beneficial effect of roots on enhancing slope stability is well recognised (e.g., Lobmann et al., 2020, Ng et al., 2021; 2022).

The fully-coupled 3D analyses presented here were performed with PLAXIS 3D (Bentley Systems, 2022), employing a user-defined soil model (Taborda et al., 2023a, 2023b), placing emphasis on both the strength and stiffness of London clay, where the Newbury cut was excavated. As explained, the model disregards the effect of roots on the mechanical and hydraulic soil properties and the presence of vegetation is accounted for through an appropriate hydraulic boundary condition. The numerical results provide insight into the mechanisms and interactions taking place during vegetation management and provide guidance as to which approaches to vegetation management may be beneficial and which should be avoided.

Problem description

Geometry, soil stratigraphy and FE discretisation

The in-plane geometry of the cut slope was typical of cut slopes in London clay, with a depth of 10m and a slope of 2:1 (horizontal:vertical) and can be seen in Figure 1. The top 3m of the 50m deep layer of London clay were considered to have been naturally weathered (Smethurst et al. 2012) and the chalk bedrock underlying the London clay layer was not considered in the numerical model and was replaced by appropriate boundary conditions, as explained later.

The 3D FE mesh used in the analysis extended 100m in the out-of-plane direction and is shown in Figure 2 (a). Figure 2 (b) illustrates an in-plane view zoomed-in around the excavation. Although the elements that were excavated at the beginning of the analysis were also included in the FE mesh, they are not shown in Figure 2 for reasons of visual clarity. The mesh consisted of 10-noded tetrahedral 3D solid elements, each node being assigned three displacement degrees of freedom in the three orthogonal directions and a pore water pressure degree of freedom. The mesh was refined behind the cut slope where a failure mechanism may develop, to accommodate the large changes in displacements and stresses expected in such an event.

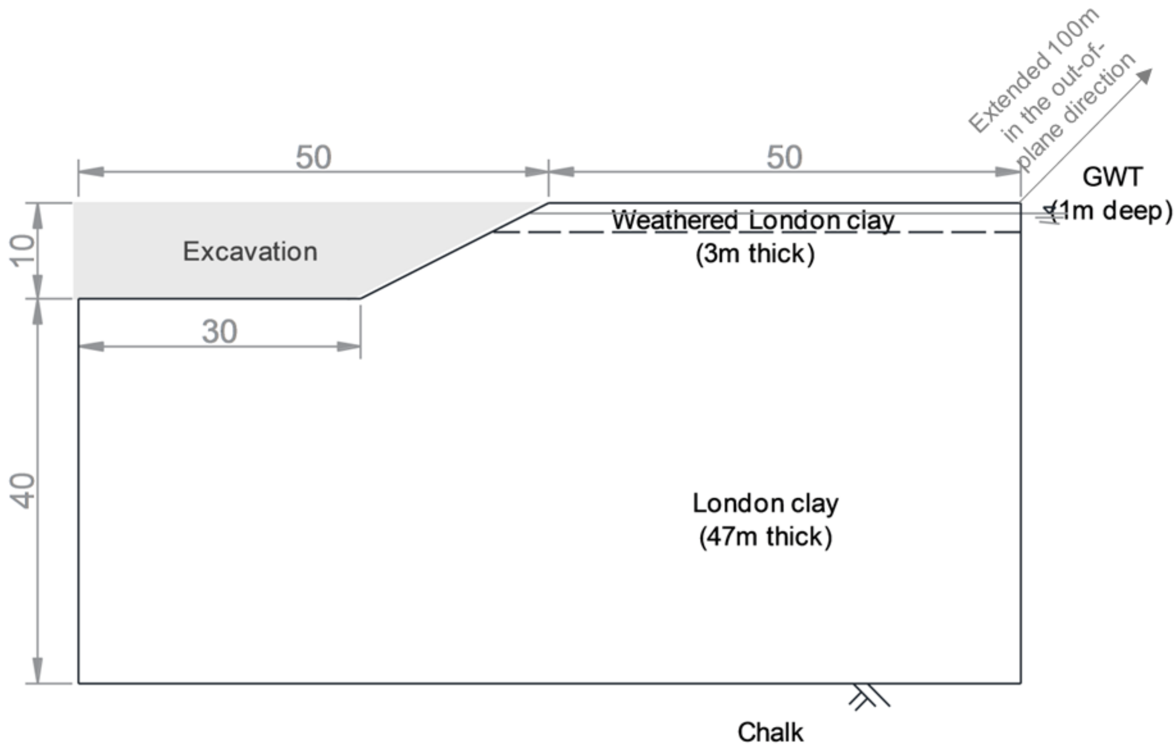

Figure 1: In-plane problem geometry and soil stratigraphy

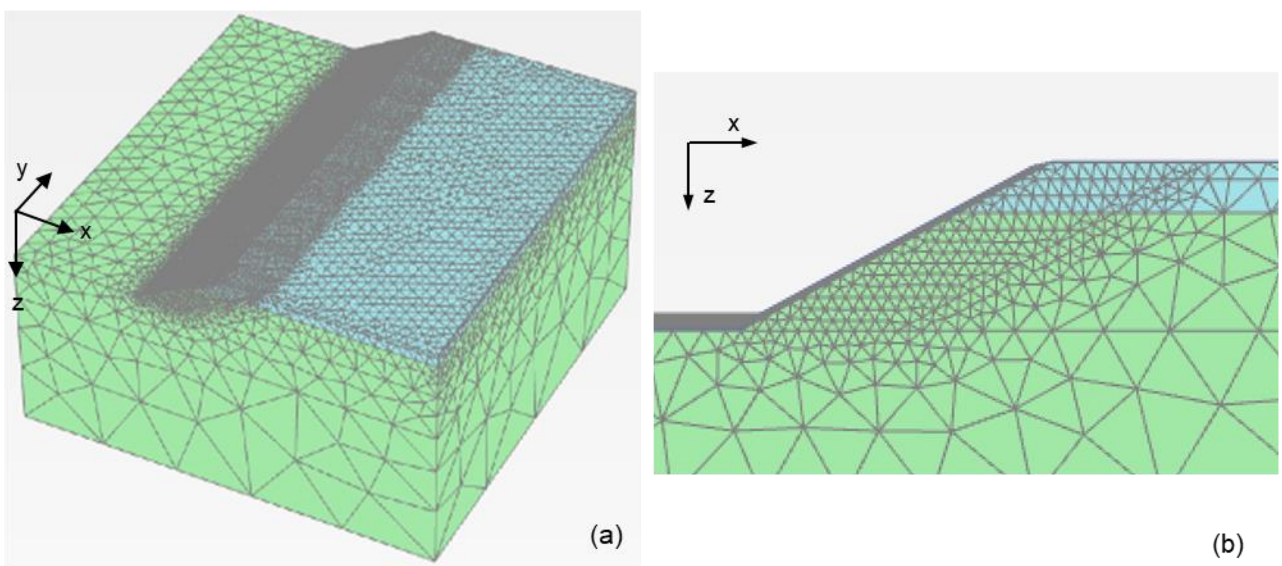

Figure 2: (a) 3D view of the adopted FE mesh; (b) zoomed-in (nearly) in-plane view of the area behind the slope

Soil properties and initial stresses

The modelling of the unweathered and weathered layers of London clay differs in relation to their hydraulic behaviour. The unweathered layer was considered to remain fully saturated under the range of suctions expected in the analysis, as London clay can withstand suctions as high as 1000 kPa before desaturating (e.g., Dias et al., 2023). To reduce the computational cost, a constant value of permeability equal to 3.47E-9 m/sec was adopted. This value reflects the average operational value of permeability adopted by Tsiampousi et al. (2017) at a depth of 10m, i.e. equal to the excavation depth. As a failure mechanism would potentially initiate from the toe of the slope (Potts et al., 2009) and as serviceability was examined in relation to an engineering asset (e.g., railway, highway) at the bottom of the excavation, this choice was deemed appropriate.

The weathered layer was allowed to desaturate with suction and follow the soil-water retention curve shown in Figure 4, which was based on interpreting field measurements of suction and water content by Smethurst et al. (2012). A version of the monotonic van Genuchten (1980) retention curve, which is readily available in PLAXIS 3D and which does not account for the effect of void ratio, was employed and its equation is given here for clarity:

$$S(\psi) = S_{res} + (S_{sat} - S_{res}) \cdot [1 + (g_a \cdot |\psi|)^{g_n}]^{\left(\frac{1-g_n}{g_n}\right)} \quad (1)$$

$S(\psi)$ is the current degree of saturation, corresponding to the current value of $\psi = -\frac{p_w}{\gamma_w}$, p_w being the suction and γ_w being the unit weight of the pore fluid. S_{sat} and S_{res} are the saturated and residual degrees of saturation, respectively, and g_a and g_n are fitting parameters similar (but not equal) to parameters α and n in the original paper by van Genuchten (1980). The values adopted to reproduce the curve in Figure 4 are summarised in Table 2.

A variable permeability model, also readily available in PLAXIS 3D, was employed to model the variation of relative permeability, $k_{rel}(S)$, with the effective degree of saturation, S_{eff}:

$$S_{eff} = \frac{S(\psi) - S_{res}}{S_{sat} - S_{res}} \tag{2}$$

$$k_{rel}(S) = \left(S_{eff}\right)^{g_l} \cdot \left\{1 - \left[1 - \left(S_{eff}\right)^{\frac{g_n}{g_n - 1}}\right]^{\frac{g_{n-1}}{g_n}}\right\}^2 \tag{3}$$

where g_l is a fitting parameter. The actual permeability can be calculated by multiplying the saturated value of permeability by $k_{rel}(S)$. Equation 3 is similar to the Mualem (1976) expression, if $g_l = 1/2$. The value adopted in the analyses is also shown in Table 2. $k_{rel}(S)$ varies between 1 and a minimum value of 10^{-4} set by the program in order to stop the actual permeability from obtaining near zero values, which could cause numerical non-convergence.

The constitutive model by Taborda et al. (2023a), which combines the Mohr-Coulomb failure criterion with the Taborda et al. (2016) small-strain stiffness model, was used to simulate the mechanical behaviour of the clay. This is not a standard feature of PLAXIS 3D and was implemented into the software as a user-defined soil model (see Taborda et al. (2023a, 2023b) for details). The same model parameters (Table *1*) were adopted for the unweathered and weathered London clay and were calibrated on London clay data from O'Brien et al. (2004) (bulk and shear stiffness moduli and their strain-level dependency, Figure 3) and Kovacevic et al. (2007) (drained shear strength)[1]. The beneficiary effect of suction is taken into account through the change in mean effective stress. The fully saturated model by Taborda et al. (2023a) was deemed appropriate to simulate the mechanical constitutive behaviour of London clay, primarily because of its nonlinear elastic stiffness, which depends on both the stress and the strain level. Not only its air-entry value of suction exceeds the suction levels obtained in the analysis, London clay is a highly overconsolidated clay, with values of overconsolidation ratio exceeding 6-7, meaning that features of unsaturated behaviour such as wetting-induced collapse would anyway be irrelevant (note also that there is further unloading because of the simulated excavation).

[1] Explanation of model parameters can be found in the supplementary file.

Furthermore, since strength is of importance in factor of safety calculations, it was necessary to avoid employing critical state type models which highly overpredict the soil strength on the dry side of critical state (Tsiampousi et al., 2013a).

The unit weight of the two layers was 19.1 kN/m^3 both above and below the groundwater table, which was assumed to be at a depth of 1m. The initial pore water pressure distribution with depth was hydrostatic and the coefficient of earth pressure at rest K_0 was 2.1, consistent with the high values of overconsolidation ratio (e.g., Hight et al., 2007).

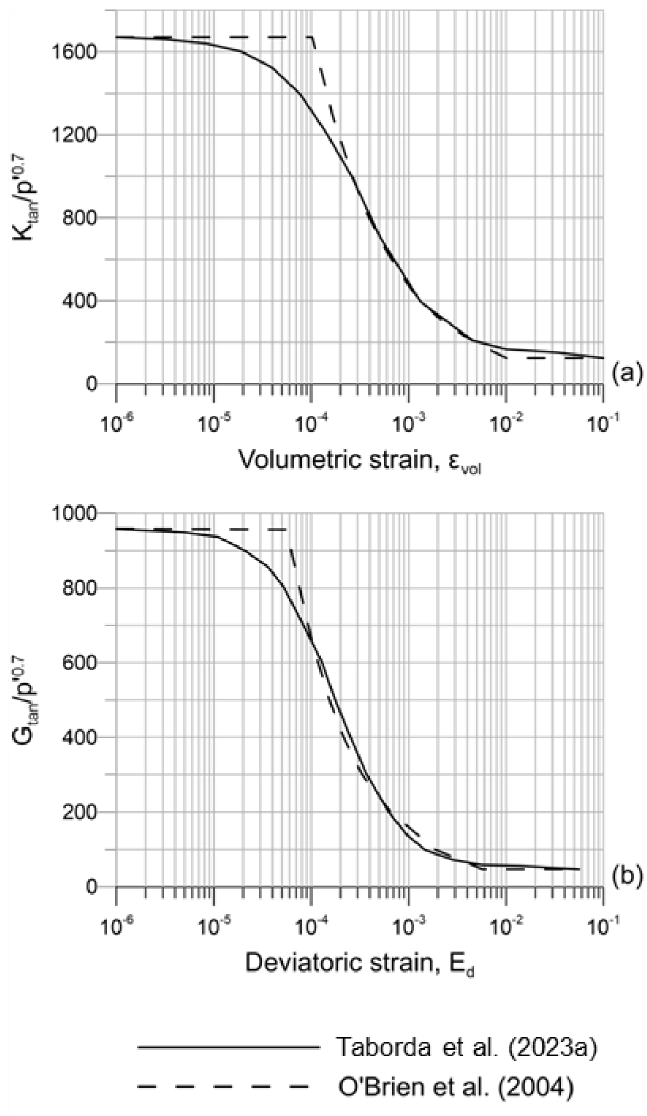

Figure 3: Degradation of (a) Bulk stiffness with volumetric strain and (b) of Shear Stiffnesses with deviatoric strain (adapted from Tsiampousi et al., 2017)

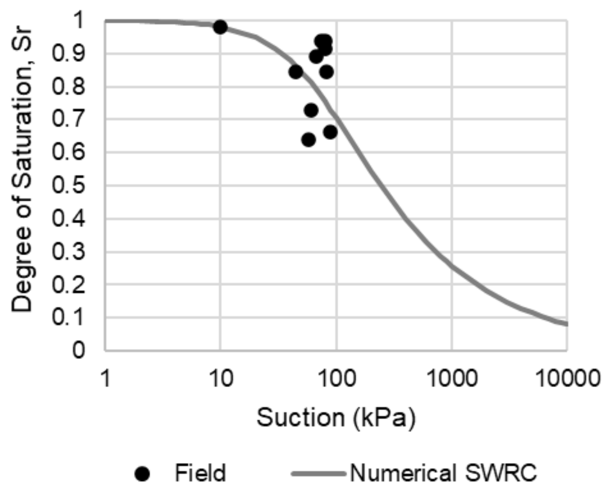

Figure 4: Soil-water retention curve for the weathered layer; field data interpreted from Smethurst et al. (2012)

Analysis sequence and boundary conditions

The excavation was performed in an undrained manner at the beginning of the analysis, in five phases in each of which a 2m deep soil layer was excavated. The subsequent phases of the analysis modelled soil-atmosphere interaction for five years and were fully coupled: the slope and the horizontal ground behind the crest of the slope were covered in high water demand (HWD) vegetation, whereas the newly formed boundary at the bottom of the excavation, hosting the engineering asset, remained bare. This five-year period aimed to reproduce repeatable year-on-year pore pressure regimes for each of the twelve months of the final two years[2], and therefore, representative conditions at the initiation of vegetation management, which was studied in detail in Year 6.

Conditions during Years 1 to 5 were equivalent to plane strain. 3D effects were introduced in the 6^{th} year of the analysis, when different vegetation management scenarios were considered,

[2] See supplementary file for pore water pressures

ranging from vegetation clearance to replacing HWD vegetation with lower water demand (LWD) vegetation at different areas and patterns on the slope. The way different types of vegetation were simulated in the analysis is a of great importance, as they affect the pore water pressures in the slope and by extension its stability and serviceability.

The infiltration boundary condition in PLAXIS 3D was used to simulate soil-atmosphere interaction. This is a dual boundary condition, changing automatically from applied inflow/outflow with a user-prescribed rate to a user-prescribed head condition and vice versa. This requires that rainfall and evapotranspiration rates are manually combined prior to inserting a single net value to be applied in the analysis. Average long-term monthly climate data, extracted from Smethurst et al. (2012) and shown in Figure 5, were used to calculate the net rates that were applied on the flat ground covered by HWD vegetation. Note that rainfall and evapotranspiration rates in Figure 5 are both plotted as positive to facilitate visual comparison, whereas net rates are shown as positive when referring to inflow and as negative when referring to outflow. The climatic year applied started in April (beginning of the “dry” season) and finished in March (end of the “wet” season).

Following the assumption made by Tsiampousi et al. (2017), a drainage system capable of capturing and removing 50% of the rainfall was present in the slope. For simplicity, and for directly comparing the effect of lowering water demand, no further changes in rainfall rates were applied (e.g., due to leaf intercept). Smethurst et al. (2012) estimated the potential evapotranspiration to be 25% less on the Newbury slope than what they calculated for a flat open site. The same reduction as a percentage was assumed here. The adjusted rates corresponding to sloping ground are also shown in Figure 5.

At the flat ground behind the crest of the excavation, the maximum possible head was set to -1m (or ~10 kPa of suction) to maintain the position of the initial water table, as field data have shown that total loss of suction is unlikely (e.g., Smethurst et al., 2012; Smethurst et al., 2015). On the sloping ground, however, the maximum possible head was set to 0m (or 0kPa of pore water pressure), so that no suctions were maintained artificially at areas where stability may be critical. The minimum possible head was set equal to -150m (or ~1500 kPa of suction) for the whole vegetated area (flat or sloping ground) and agrees with previous values reported in the literature (e.g., Nyambayo & Potts, 2010).

As explained in the next section, different vegetation management scenarios were considered where HWD vegetation was either removed or replaced by LWD vegetation. To simulate vegetation removal from the slope, the potential evapotranspiration rates were reduced to 10% of those applied on the slope when it was covered in HWD vegetation, while the slope rainfall rates remained unchanged. This would qualitatively reflect evaporation conditions on a north-facing slope (which would be the critical one). A similar process was followed when calculating the net rates corresponding to LWD vegetation, with the difference that the evapotranspiration rates were reduced to 50% rather than to 10%. The same rates had been assumed by Tsiampousi et al. (2017).

Throughout the fully coupled phases of the analysis, seepage was allowed at the bottom of the excavation, where the engineering asset is located. Suctions generated during the undrained excavation could dissipate through this boundary, but water could not pond on it. All vertical boundaries were impermeable (planes of symmetry), with the exception of the right-hand-side out-of-plane vertical boundary, where seepage was allowed and pore water pressures changed in response to the applied inflow/outflow rate at the top boundary of the FE mesh. Pore water pressures were left unchanged at the interface with the permeable chalk at the bottom boundary. The horizontal displacements at the four vertical boundaries and the horizontal and vertical displacements at the bottom boundary were fixed throughout the analysis.

As explained above, the analysis is loosely based on the case study of the Newbury cut slope (Smethurst et al., 2012), which had previously been used to validate the numerical methodology adopted here (e.g., Tsiampousi et al., 2017; Tsiampousi et al., 2023b). This methodology is expanded here to a generic 3D hypothetic case, as vegetation management scenarios such as the ones adopted in the analyses have not yet been trialled in the field.

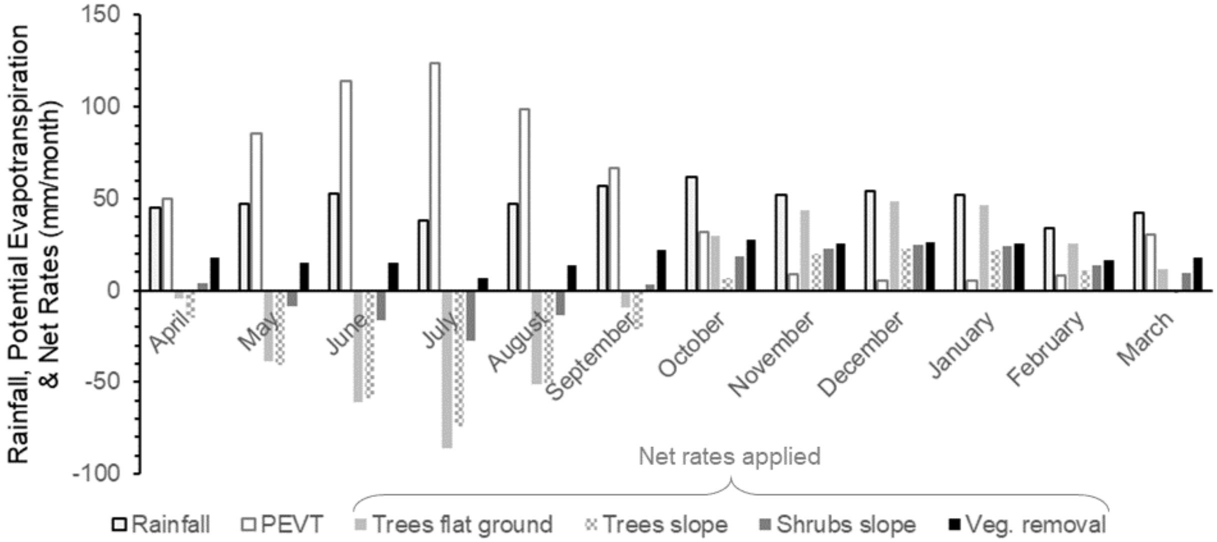

Figure 5: Precipitation, potential evapotranspiration and net rates for a typical year (negative values of net rates indicate that potential evapotranspiration exceeds precipitation rates)

Cases considered

Ten different scenarios of vegetation removal, where HWD vegetation was removed leaving only low and sparce vegetation behind, and vegetation replacement, where HWD was replaced by LWD vegetation, were considered during the 6th Year of the analysis, which was dedicated to vegetation management. They are shown schematically in Figure 6, which illustrates a plan view of the slope, where vegetation management was applied. The boundary conditions on the remaining of the FE mesh, including on the flat ground behind the crest of the slope, were left unchanged.

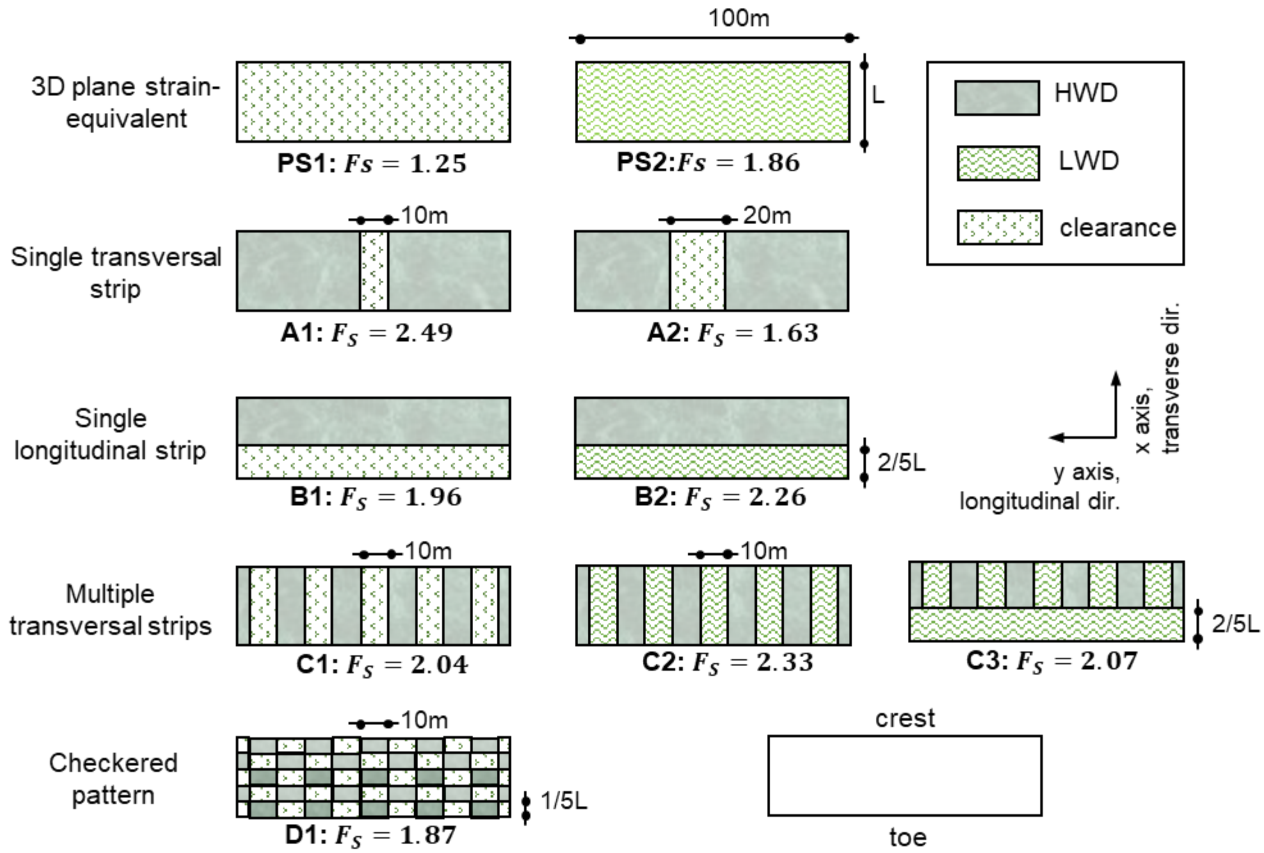

Figure 6: Schematic reproduction of the vegetation management scenarios PS1-2, A1-2, B1-2, C1-3 and D1; plan view of the slope (see sketch at bottom right for orientation).

Factor of safety

The factor of safety (FoS) against failure was calculated at the end of Year 6 in each of the analyses in order to capture the FoS and the corresponding failure mechanism at the end of the wet period, after one year of vegetation management. The FoS phases of the analyses were drained meaning that pore water pressures were not allowed to change as per previous analyses (e.g., Tsiampousi et al., 2013b; Tsiampousi et al., 2016; Tsiampousi et al., 2017). A c'/φ' reduction technique, which applies partial factors of safety on cohesion and the tangent of the angle of shearing resistance until failure is achieved, was implemented within the user-defined constitutive model and its integrator for the purposes of this study. Failure was manually verified in each case by examining whether a failure mechanism was fully developed by assessing vectors of incremental displacements. FoS are reported to an accuracy of 2 decimal places. This bears little engineering significance, a fact which should be accounted for when evaluating the analysis results, and was done for theoretical consistency between the reported FoS and the corresponding failure mechanism: e.g., a number of analysis steps were carried out between FoS of 1.6 and 1.63 in A2 (see Figure 6) in which the failure mechanism evolved towards its final shape and location.

Effect of HWD vegetation on slope serviceability

Before exploring vegetation management, the impact of current vegetation on the serviceability of the slope was established through careful examination of the displacements computed in the first 5 years of the analysis, simulating the presence of HWD vegetation on the slope. This phase of the analysis was common for all ten vegetation management scenarios considered, meaning that all subsequent results could be benchmarked against the results of this phase.

Figure 7 shows the total vertical displacements at the bottom of the excavation along a line perpendicular to the slope toe in August and March of Year 5 in comparison to the vertical displacements at the end of the undrained excavation. This monitored line would be perpendicular to the axis of the engineering asset. Until Year 5 the analysis is essentially equivalent to plane strain and therefore the exact location of this line along the y-axis (longitudinal direction) is irrelevant. In the present case, for simplicity, a line in the middle of the model (at y = 50m) was selected.

It can be observed that the vertical displacements at the end of the excavation showed little variation along the monitored line. Their magnitude is associated to the short-term unloading taking place. Note that in this undrained part of the analysis, the overall soil volume remained unchanged, and the local displacements seen here were compensated for elsewhere in the FE mesh to produce a net zero volume change.

By the end of August of Year 5, heaving had occurred at the centre of the excavation (x = 0m) and shrinkage at the toe (x = 30m). The former was due to the dissipation of tensile excess pore water pressures that developed during the excavation (swelling), whereas the latter was associated with the action of vegetation on the slope during the dry period, when evapotranspiration exceeds rainfall, and a net outflow is obtained. A large differential displacement, in excess of 120 mm, is obtained as a result. This would be a significant differential displacement for an engineering asset, in particular for a railway. By the following March, swelling had occurred in relation to August, which was larger around the toe than at the centre, hence reducing the magnitude of the differential displacements to about 100 mm, which was still significant.

The analysis results clearly underline the need for vegetation management in slopes covered in HWD vegetation. When the entire slope was cleared of its vegetation in PS1 (see Figure 6), the FoS one year later had reduced to 1.25 from 2.6 at the end of Year 5. In agreement with what has already been observed in the literature (Smethurst et al., 2015; Tsiampousi et al., 2017), simply clearing vegetation has the potential to alter a serviceability problem into a stability problem. Therefore, both stability and serviceability need to be considered while managing vegetation.

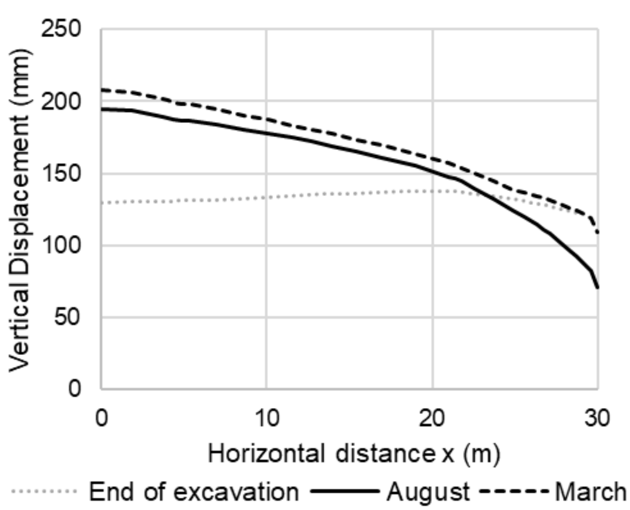

Figure 7: Vertical displacements at the bottom of the excavation along a line perpendicular to the toe at y = 50m for Year 5; x = 0m corresponds to the centre of the excavation, x = 30m corresponds to the toe of the slope

Width of vegetation removal

The aim of analyses A1 and A2 was to establish what effect the width of vegetation removal has on the stability of the slope in order to adopt a reasonable value in the subsequent analyses which were devoted in studying vegetation management under 3D conditions.

The FoS prior to vegetation removal, i.e., at the end of the wet period (March) of Year 5, was calculated to be 2.6. The FoS at end of March of Year 6, i.e., following vegetation clearance, reduced to 2.49 for scenario A1 and 1.63 for scenario A2 (see also Figure 6). The corresponding failure mechanisms are shown in Figure 8. It should be noted that it is the relative and not the actual magnitude of the vectors of incremental displacements that is of interest, as this is what demonstrates the existence of a failure mechanism. It is evident that the failure mechanism for a 10m wide clearance strip (A1) was significantly deeper than the mechanism for a 20m wide clearance strip (A2). In the latter case, the mechanism was limited to the toe of the slope, whereas in the former this was not the case, and a much deeper area of the FE mesh was mobilised.

To investigate the longitudinal extent of the failure mechanism in the y-direction, the transverse incremental displacements (i.e., the displacements in the x-direction) were examined for the failure step. Figure 9 illustrates the incremental transverse displacements along the toe of the slope for the two scenarios, normalised by the maximum absolute value. For scenario A2, the failure mechanism was centred about the centre of the clearance strip (y = 55m) and was contained within its 20m width, in that the transverse displacements were zero outside the 45 – 65m y co-ordinate. For scenario A1, the soil along the whole longitudinal extent of the mesh in y-direction was mobilised, with displacements being the largest within the 10m wide clearance strip (centred at y = 50m) but not limited to within the width of this strip.

Figure 10 shows contours of suctions at the end of March of Year 6 on the slope (top views in (a) and (b)) and at cross sections at the centre of the respective clearance strips and 10m away ((c) to (f)), for scenarios A1 and A2. From the top views ((a) and (b)), it is evident that vegetation clearance affected primarily the suctions at the clearance strip, and, to a much lesser extent, outside it, with the biggest affect outside the strips concentrated at the bottom half of the slope and in the vicinity of the strips. Although there were some small differences in the values and shapes of contours at the central cross-sections for A1 and A2 ((c) and (d)), the differences were more significant in the cross-sections located 10m away from the centre of the strip ((e) and (f)), with A1 having resulted, unsurprisingly, to higher suctions. These higher suctions 10m away from the centre of the clearance strip in A1 aided the soil to resist the full development of a failure mechanism, mobilising the shear strength of areas further away. Nonetheless, the suctions further away are equally large and become progressively, albeit slightly, larger, impeding the formation of a fully developed failure mechanism. This explains why transverse displacements at the last step of the FoS analysis were non-zero even at y = 0 and 100m (Figure 9) and why the calculated value of F_S (2.49) was only slightly smaller than the value of F_S (2.6) at the same month (March) prior to vegetation clearance.

The results of analyses A1 and A2 indicated that although a single 20m wide clearance strip was wide enough for a fully developed failure mechanism to develop within it, with a significant reduction in FoS, a single 10m wide clearance strip was narrow enough to avoid a failure mechanism developing within it, mobilising the strength of soil in areas still covered in HWD vegetation. This observation supports the choice of 10m wide strips when studying vegetation clearance in scenarios C1 and D1, but also when considering vegetation replacement in scenarios C2 and C3, to allow for direct comparison between cases.

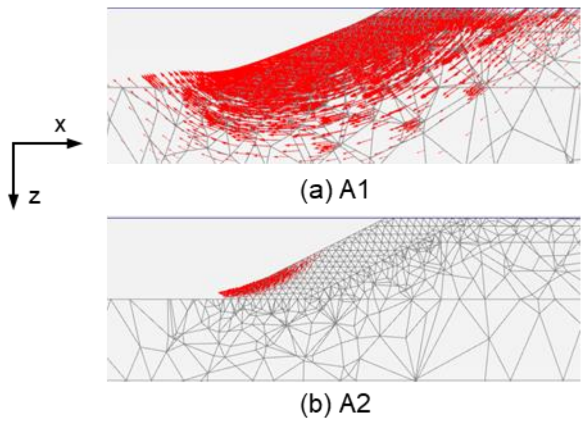

Figure 8: Vectors of incremental displacement at failure for scenarios A1 and A2

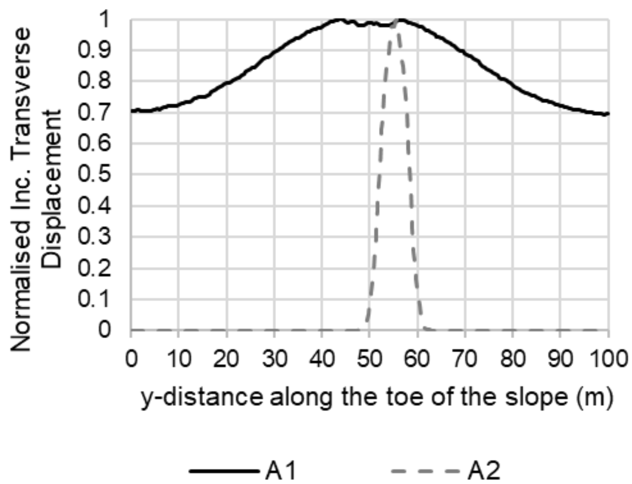

Figure 9: Normalised incremental transverse displacement (i.e., in the x-direction) along the toe of the slope for scenarios A1 and A2

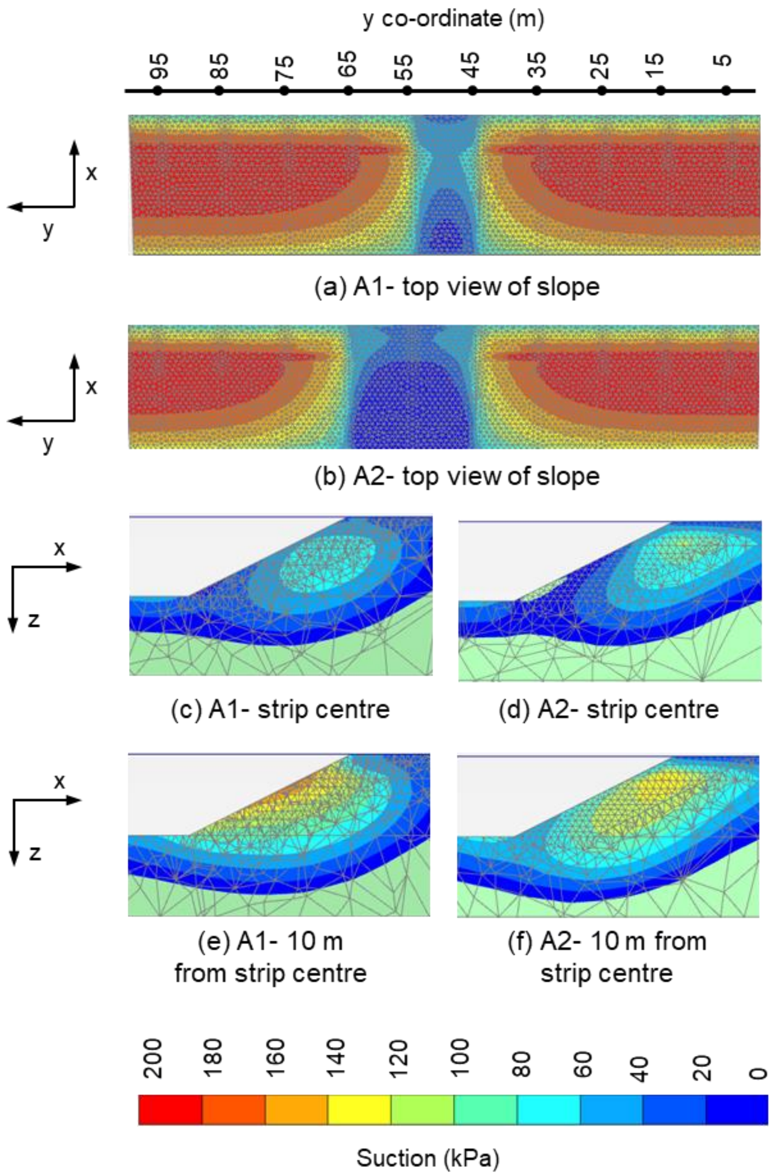

Figure 10: Contours of suction (kPa)

Stability

Vegetation removal

The FoS for scenarios B1, C1 and D1 simulating vegetation removal have been included in Figure 6. The respective failure mechanisms at the last converged step of the FoS analyses are shown in Figure 11 (a) to (c). The failure mechanisms extended longitudinally to the whole width of the

FE mesh, owing either to conditions being equivalent to plane strain (B1) or to the closely repeated pattern of vegetation (C1 and D1).

With particular reference to C1 in relation to A1, the FoS reduced visibly when multiple 10m wide strips were considered. It was seen that the single strip in A1 was not of adequate width for a failure mechanism to fully develop within it, mobilising the shear strength of the soil in areas outside it. The longitudinal extent of these areas on either side of the single strip in A1 exceeded by far the 10m width of the vegetated strips in C1 which remained intact between the cleared strips (Figure 9), which explains the reduction in FoS.

All three cases, B1, C1 and D1, yielded a FoS which was larger than PS1 (also summarised in Figure 6), indicating that maintaining some HWD vegetation on the slope is beneficial for its stability. C1, which resulted in the deepest failure mechanism, also resulted in the largest FoS. This is perhaps not surprising when comparing C1 to B1, as in C1 HWD vegetation is still present intermittently at the toe, where failure initiated in the analysis, increasing overall the pore water pressures, whereas in B1 HWD vegetation was cleared entirely from the toe. Interestingly, this pattern was not observed in D1, which produced the smallest FoS and where HWD vegetation was also present intermittently at the toe, albeit at a different pattern than in C1. Considering an in-plane (i.e., transversal to the slope) cross-section, the failure mechanism initiated at the toe and propagated upwards with increasing partial factors of safety. Continuous presence of HWD vegetation (i.e., increased pore water pressure) in regularly repeated in-plane cross-sections in C1 provided extra in-plane stability at these cross-sections. This was not the case in in-plane cross-sections in D1, where there was no continuity of HWD vegetation. Continuous presence of HWD vegetation at the upper part of the slope in B1 also assisted in-plane stability in comparison to D1, albeit to a lesser extent than in C1.

Following vegetation clearance, slope stability was enhanced by the presence of HWD vegetation at the toe, even when this was intermittent in the out-of-plane (longitudinal) direction, as long as there was continuity of HWD vegetation in in-plane cross sections, which were equally spaced in this particular case. Further checkered patterns were not considered (e.g., for vegetation replacement), as they would be mechanically, as well as economically (e.g., increased cost of maintenance of this elaborate pattern), of low interest.

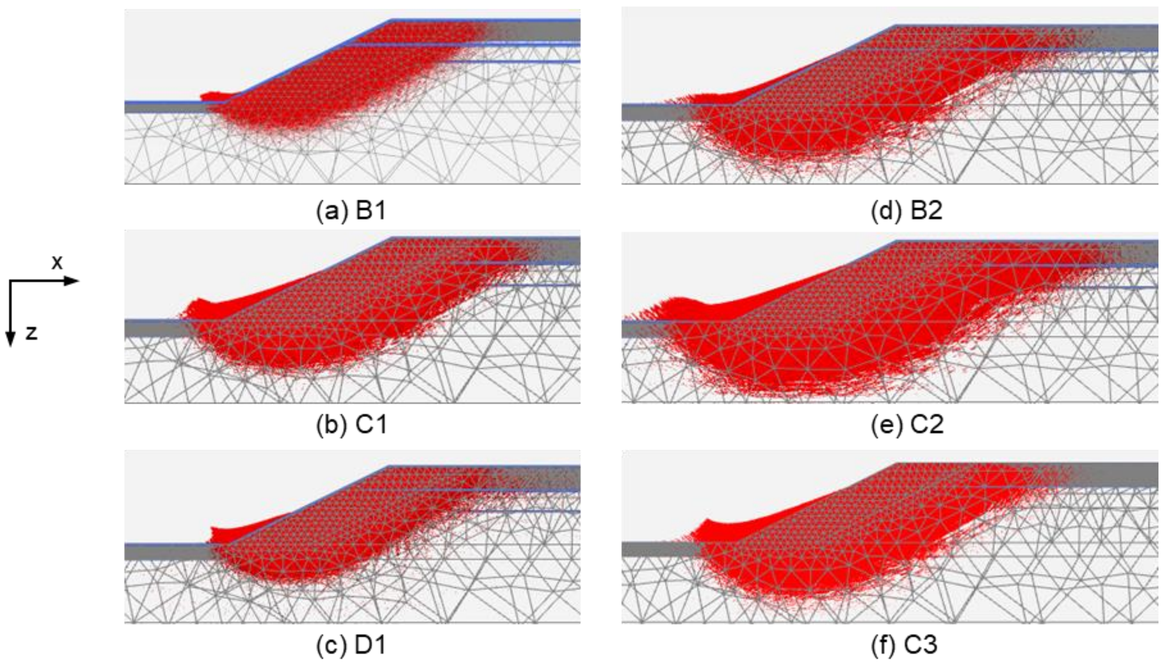

Figure 11: Vectors of incremental displacement at failure

Vegetation replacement

The FoS for scenarios B2, C2 and C3 simulating vegetation replacement can be found in Figure 6 and the respective failure mechanisms in Figure 11 (d) to (f). All three cases yielded a FoS which was larger than PS2, indicating again that maintaining some HWD vegetation on the slope is beneficial for its stability. A similar relationship between B2 and C2 in terms of calculated FoS was obtained as for B1 and C1, indicating that conclusions drawn from the vegetation clearance exercise can be extrapolated to vegetation replacement, with particular reference to the presence of HWD vegetation at the toe. This is further supported by the lower FoS computed for C3, which combined absence of HWD vegetation at the toe and intermittent present of HWD vegetation at the upper part of the slope and produced the lowest FoS out of the three vegetation replacement analyses. When compared directly to their respective vegetation clearance scenarios, the vegetation replacement scenarios B2 and C2 yielded higher FoS and deeper failure mechanisms. This is of course expected, as LWD vegetation potentially maintains higher suctions through evapotranspiration than in the case of vegetation clearance, which is reflected in the net rates that have been applied in the analyses (Figure 5). The FoS for C3, although smaller than for other vegetation replacement analyses, was comparable to the highest FoS for vegetation clearance (C1), indicating that replacing rather than clearing vegetation may generally be a better option, not only for enhancing biodiversity, but also for the stability of the slope irrespective of the actual pattern followed, as long as some continuity of HWD vegetation in in-plane cross-sections is maintained. Nonetheless, replacing vegetation would be a more expensive approach to vegetation management than clearing vegetation, and one requiring further resources (e.g., frequent but careful irrigation during plant growth season, until the new vegetation gets established). Furthermore, its impact on serviceability in comparison to vegetation clearance also needs to be taken into account.

Serviceability

Vegetation removal

The vertical displacements computed for the vegetation removal scenarios at the bottom of the excavation perpendicular to the slope toe are shown in Figure 12 (a) for August and in Figure 12 (b) for March of Year 6 and are compared with the corresponding displacements from Year 5. For B1 and D1, the monitoring line was at y = 50m, and for C1 at y = 60m, coinciding with the centre of a HWD vegetated strip, where, as discussed subsequently, the differential displacements were the largest.

Starting with August, further swelling occurred between Years 5 and 6. The removal of HWD vegetation reduced the shrinkage at the toe in all three vegetation management analyses, with the vertical distance of the respective curves from the curve for Year 5 being larger at the toe of the slope (x = 30m) than at the centre of the excavation (x = 0m). As a result, the differential displacements between the toe and the excavation centre reduced from 120mm to roughly 75, 110 and 100 mm, in B1, C1 and D1, respectively.

Although B1 seemed to lessen the serviceability problems by 37.5% in August (by 45mm out of the initial 120), in March upward vertical displacements accumulated at the toe as a result of the increased rainfall infiltration following HWD vegetation removal from the entire longitudinal strip along the toe. If the width of the asset is significantly smaller than the width of the excavation and it is centred around the centreline of the excavation, serviceability will have improved. If, however, the whole width of the excavation is made use of to host the asset, then serviceability at the edge of the excavation has markedly deteriorated. A similar upward displacement close to the toe in relation to March of Year 5 can also be observed for D1, albeit significantly smaller in magnitude. This can be explained by the partial, rather than total, removal of HWD vegetation from the toe, which contributed to the overall pore water pressures around the slope remaining higher than in B1. Despite the swelling that occurred around the toe for C1 between August and March, this was not as significant as in B1 and D1. It would be difficult to differentiate the effect of swelling at the toe because of decreasing suctions during the wet period following vegetation clearance, from the effect of reducing stiffness due to reducing effective stresses and due to shearing (note the difference in FoS in the three analyses, which signifies that the FoS calculation phase started from significantly different stress states). It is likely that the displacements at the toe are a combination of all these interacting mechanisms in these coupled consolidation analyses, where stiffness was a function of both stress and strain.

The vertical displacements in Figure 12 are presented normalised in Figure 13 for further comparison. The normalisation presented refers to the maximum value of Δdisplacement/Δx for each curve, i.e., is a worst-case scenario sort of slope. A reduction in the normalised vertical differential displacement signifies an overall improvement in serviceability. With reference to the August results, B1 produced the largest improvement between the three vegetation clearance scenarios (B1, C1 and D1). However, the same analysis yielded the worst results for March. The improvement for C1 was less significant in August (when the serviceability issues are more critical) than in March. For D1 there was hardly any improvement in March, and the improvement was more significant in August.

To put these displacements into perspective, the cross-level maintenance tolerance in high cant deficiency curves is set by Network Rail (2022) in the UK to 10 mm (cross-level refers to the difference in elevation between tracks). Considering that track gauge is typically 1,435 mm, this gives a normalised ratio equivalent to that plotted in Figure 13 of just 6.97. It should be highlighted that there is no direct relationship between ground movements and track geometry, the track geometry being used in Network Rail standards for both design and maintenance, and therefore comparison between this value and the values in Figure 13 is only indicative of the potential significance of the computed displacements.

Figure 14 plots the transversal, longitudinal and vertical displacements (in the x- and y- and z-directions) displacements in August for C1 and D1 along the toe of the slope (note that B1 is an equivalent plane-strain analysis, therefore, yielding uniform displacements in the out-of-plane). Perhaps unsurprisingly considering the extent of the HWD vegetated zone up the slope in the two cases, the differential displacements were larger for C1 than D1. The magnitudes of the differential displacements (marked in Figure 14) may not seem very large. However, the longitudinal and transversal differential displacement, in combination with the prevalence of evapotranspiration during August, may contribute to desiccation cracking and increased inflow of rainfall water during the next wet period, exacerbating the seasonal changes of pore water pressures year-on-year, and therefore, further contribute to poor serviceability. The vertical differential displacements occur within a distance of 10m, so in normalised terms they are comparable to the differential displacements in Figure 12. This may or may not be acceptable, depending on the nature and geometry of the engineering asset, but it should be noted that differential displacements tend to become progressively worse with time, and therefore, while attempting to solve serviceability issues perpendicular to the asset axis, the approach in C1 and

D1 may inadvertently induce new serviceability issues along its axis, with C1 presenting a worse outcome than D1.

An indication of the significance of the calculated vertical displacements can be obtained by considering the Network Rail (2022) maintenance limits for cyclic top, i.e., for series of regularly spaced drops in the vertical alignment of the tracks, a fault which can potentially cause derailment. For example, cyclic tops of 20 to 23 mm on one rail, or 43 to 46 mm on both rails need to be corrected within 60 days. Very importantly, it is required that the trigger is also rectified to ensure that the fault does not re-occur. The wavelength for cyclic top depends on the train speed and is typically recorded at 4.5, 6, 9, 13 and 18 m, i.e., at distances relevant to the wavelength of 10 m encountered in the analysis. Similarly, to put the transversal displacements into perspective, the 35 m horizontal alignment of the track can be considered: Network Rail (2022) identifies a 30 mm intervention limit and a 25 mm maintenance tolerance. As highlighted earlier, a direct relationship between ground movements and track geometry has not been established, so these comparisons should only be seen as an indication of the relative significance of the computed ground movements.

The observed differential vertical displacements along the toe have yet another implication in the interpretation of the results. Although the minimum vertical displacement for C1 was obtained at y = 60m, the minimum vertical displacement for D1 was obtained at y = 50m, coinciding in both cases with where the HWD vegetation remained untouched at the toe of the slope and contributed to local shrinkage. The transversal (in-plane) sections where the minimum vertical displacements are obtained at the toe suffer the worse serviceability issues (largest difference with centre-line vertical displacements). This has practical implications for the interpretation of the numerical results, as well as for field monitoring of differential displacements across the route of the asset, which should ideally be centred about the HWD vegetated areas.

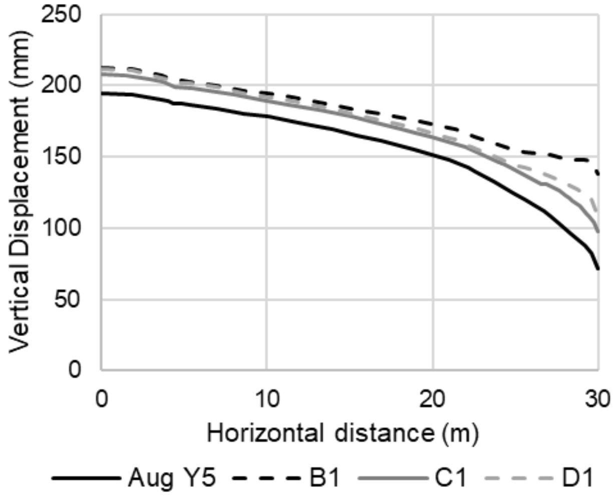

(a) August

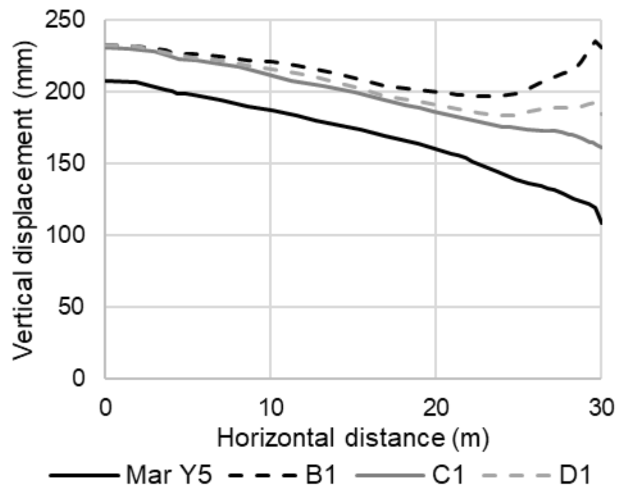

(b) March

Figure 12: Vertical displacements at the bottom of the excavation along a line perpendicular to the toe for Year 6 (at y = 50m for B1, D1 and at y = 60m for C1) in comparison with Year 5 (a) in August and (b) in March

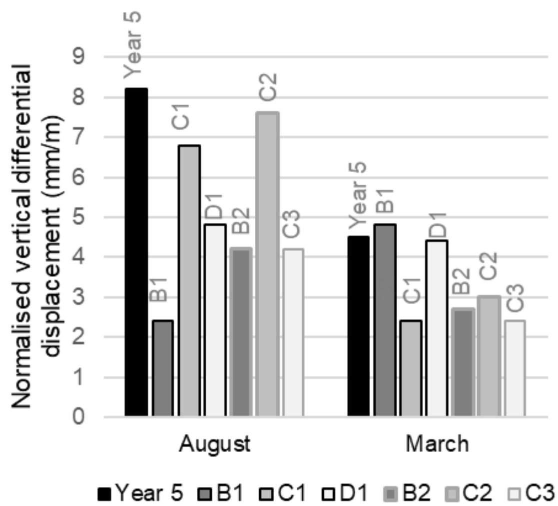

Figure 13: Normalised vertical differential displacements in August and March

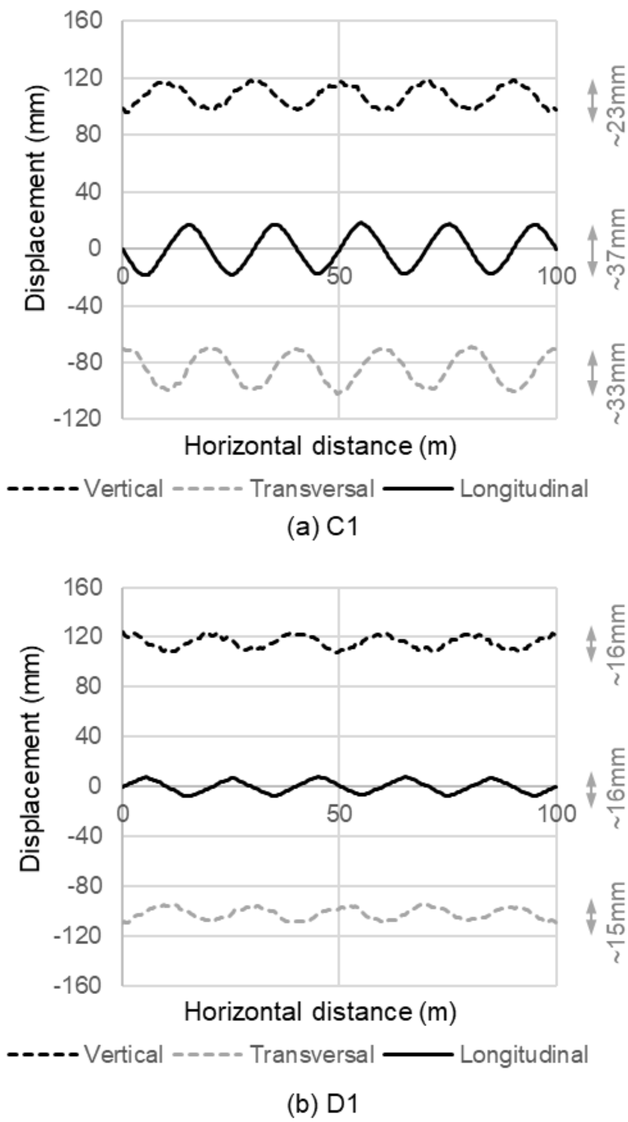

Figure 14: Transversal (x), longitudinal (y) and vertical (z) displacements along the toe for scenarios (a) C1 and (b) D1

Vegetation replacement

Figure 15 illustrates the vertical displacements perpendicular to the asset axis at y = 50m for B2 and C3, and at y = 60m for C2. The August differential displacements have improved by similar measures in B2 and C3, as also shown in Figure 13, with the displacement curves for the two analyses showing little difference. The improvement was visibly smaller for C2. By the following March, differences in the displacements for B2 and C3 became obvious close to the toe, with C3 demonstrating the highest swelling (and smallest differential displacement), owing to more HWD vegetation overall having been replaced than in B2. The benefit, however, was small and counterweighted by the reduced FoS and the increased associated cost of maintaining more complex patterns of vegetation. Overall, the March serviceability was improved by comparable measures in all three analyses.

In contrary to what was observed in B1, where in March serviceability was critical close to the toe, in B2, which was the equivalent scenario to B1 but with vegetation replacement rather than clearance, this was no longer the case. As a result, in March, serviceability was improved for B2 in relation to Year 5 (Figure 13). The serviceability of the slope improved more in C1 than in C2, i.e., for the clearance rather than the replacement scenario, both in August and in March, although scenario C1 in itself did not present an attractive solution anyway, as already discussed.

The transversal, longitudinal and vertical displacements along the toe are shown in Figure 16. Differential displacements of magnitudes comparable to, but smaller than, C1 were obtained for C2. Vegetation replacement seemed to cause smaller serviceability problems along the toe, as the difference between net inflow/outflow, and therefore, pore water pressures, for HWD and LWD vegetation, which alternate along the toe in C2, is smaller than for HWD vegetation and vegetation clearance, which alternate along the toe in C1. Removing the HWD vegetation from the bottom part of the slope in C3 prevented any differential displacements from developing, signifying that conditions along the toe were not affected by the irregular vegetation pattern higher up the slope.

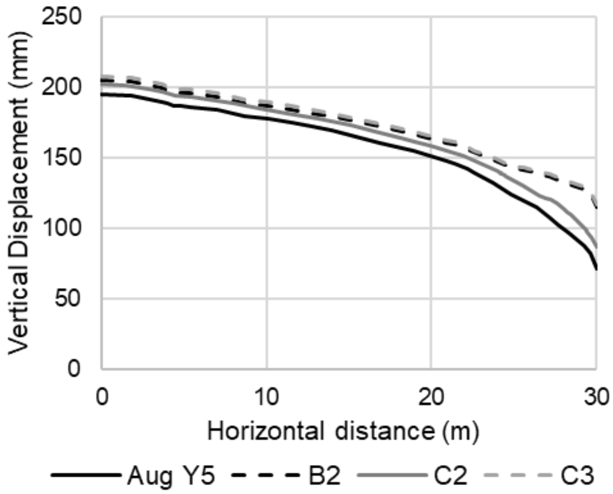

(a) August

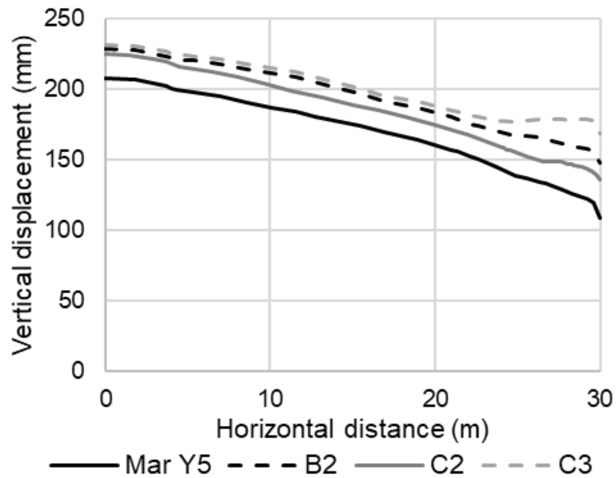

(b) March

Figure 15: Vertical displacements at the bottom of the excavation along a line perpendicular to the toe at y = 50m for scenarios B2 and C2 and at y = 60m for D2, for Year 6 in comparison with Year 5 (a) in August and (b) in March

As highlighted earlier, the displacements around the toe would be an outcome of suction reduction in combination with coupled mechanical effects, rendering it impossible to predict whether serviceability would improve or deteriorate with different vegetation management scenarios a-priori, based solely on intuition. From the analyses results presented here, it is evident that scenarios B2 and C3, that involve vegetation replacement at the toe, would yield the best all-around outcome for the slope, with serviceability improving both in August and in March and with values of F_s of above or around 2 maintained. Perhaps scenario B2 is the most attractive, considering the lower maintenance it would require and the better outcome for slope stability.

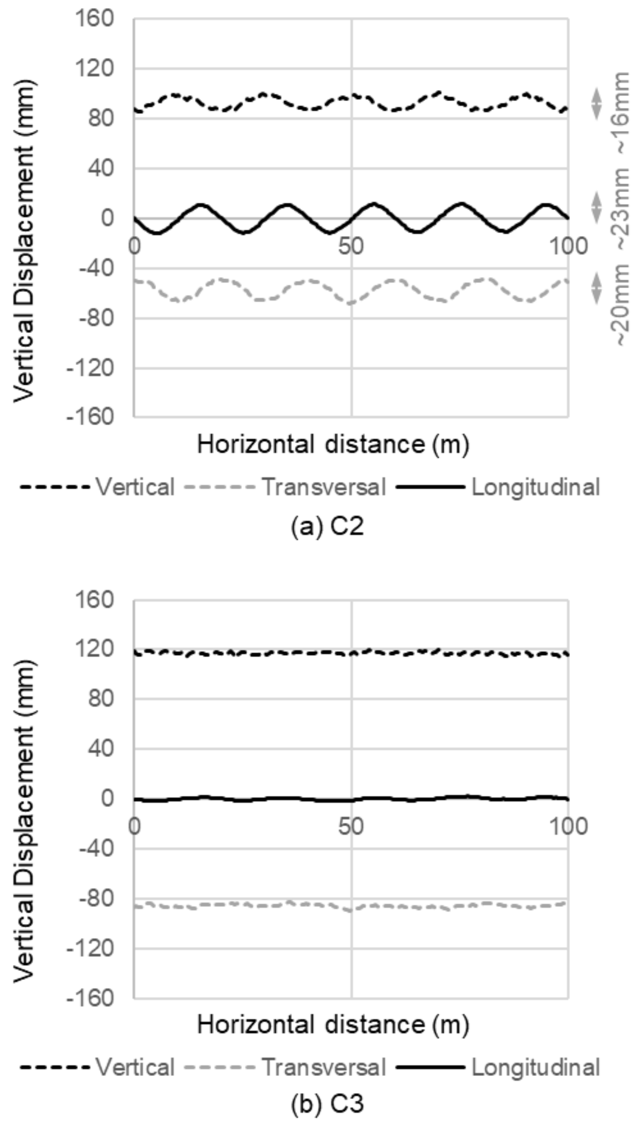

Figure 16: Vertical (z) and horizontal (x and y) displacements along the slope toe for scenarios (a) C2 and (b) D2

Conclusions

The paper studied and compared the effects of vegetation clearance and vegetation replacement on the stability and serviceability of a typical slope cut in London clay, considering various vegetation management scenarios in 3D. Although focused on a geometry and climate representative of SE England, the conclusions drawn from the study are universal, in that they account for the changing balance of pore water pressures, strength and stiffness, which qualitatively would be similar to many other cases and climates.

When considering vegetation management, the continuous presence of HWD vegetation in in-plane cross-sections may prevent to a certain extent a dramatic loss of stability, even if continuity is limited to the upper part of the slope. Maintaining some HWD vegetation on the slope is generally beneficial for its stability, and with appropriate vegetation management serviceability can be improved. Care should be taken that, while attempting to solve serviceability issues perpendicular to the asset axis, vegetation management does not inadvertently induce new serviceability issues along its axis.

Serviceability is not generally and universally improved by vegetation clearance. In certain cases, clearance may lead to a worsening serviceability, as well as to worsening stability. In fact, vegetation replacement, although potentially more expensive, may be preferrable for both reasons of stability and serviceability, as well as for enhancing bio-diversity.

From the scenarios considered here, it would seem that the preferred option may be to replace HWD vegetation along the toe of the slope with LWD vegetation. The optimal extent of vegetation replacement up the slope remains to be studied and this could be done in 2D.

It needs to be highlighted that it would not have been straightforward, and perhaps not possible, to predict based solely on intuition which scenario would provide the best combined outcome for the stability and the serviceability of the slope, post vegetation management. This is because reduced shrinkage at the toe associated with a change of inflow/outflow rates, needs to be considered concurrently with a potential reduction of stiffness and strength due to reducing suctions and, therefore, effective stresses. The complex mechanisms taking place, render numerical analysis a very useful and cost-effective tool which can be used to guide and inform field and large-scale laboratory investigations, which are of course irreplaceable but also require a lot more resources.

Further to the conclusions drawn directly from the study, the paper's contribution extends to presenting a numerical methodology and a numerical model for 3D conditions which can form the basis for further studies, such as the effect of irregular in the out-of-plane vegetation on progressive failure, the progression of serviceability with time post-vegetation management, modelling of isolated trees or group of trees on the slope and their management, to name a few. Similar methodologies can be extended to study 3D vegetation effects on natural slopes, embankment slopes, flood embankments and any other geotechnical structure that interacts with the atmosphere.

Further analyses should ideally take into account the mechanical reinforcement of the soil due to the presence of roots. This requires that a consistent and robust methodology is developed on how to incorporate vegetation replacement and clearance in constitutive models.

Numerical analysis can provide preliminary, cost-effective information and guide large-scale laboratory and field investigations, which require a lot more resources but are irreplaceable and necessary. The paper provides clear numerical evidence for the first time of the importance of considering vegetation management as a three-dimensional problem for stability as well as for serviceability and can underpin a paradigm shift in laboratory and field investigations of vegetation management on infrastructure slopes.

References

Dias, A.S., Hughes, P.N. and Toll, D.G., 2023. Soil–Water Retention Curve Prediction for Compacted London Clay Subjected to Moisture Cycles. Geotechnical and Geological Engineering, pp.1-16.

Dias, A. S., Pirone, M., Nicotera, M. V. & Urciuoli, G. (2022) Hydraulic characterization of an unsaturated vegetated soil: The role of plant roots and hydraulic hysteresis. *Geomechanics for Energy and the Environment*, **30**

Elia, G., Cotecchia, F., Pedone, G., Vaunat, J., Vardon, P. J., Pereira, C., Springman, S. M., Rouainia, M., Van Esch, J., Koda, E., Josifovski, J., Nocilla, A., Askarinejad, A., Stirling, R., Helm, P. Lollino, P & Osinski P. (2017) Numerical modelling of slope-vegetation-atmosphre interaction: an overview. *Quarterly Journal of Engineering Geology and Hydrogeology*, **50** (3), 249–270

Fraccica, A., Romero, E., Fourcaud, T., Sondon, M. & Gandarillas, L. (2020) Tensile strength of a vegetated and partially saturated soil. Cardoso R., Jommi C., Romero E. (Eds.), 4th European Conference on Unsaturated Soils - E-UNSAT2020. E3S Web of Conferences, 195 (2020), p. 03001, 10.1051/e3sconf/202019503001

Greenwood, J., Norris, J. & Wint, J. (2004) Assessing the contribution of vegetation to slope stability. *Proceedings of the Institution of Civil Engineers-Geotechnical Engineering*, **157** (4), 199-207.

Hight, D.W., Gasparre, A., Nishimura, S., Jardine, R.J., Coop, M.R. and MINH, N., 2011. Characteristics of the London Clay from the Terminal 5 site at Heathrow Airport. In Stiff Sedimentary Clays: Genesis and Engineering Behaviour: Géotechnique Symposium in Print 2007 (pp. 167-182). Thomas Telford Ltd.

Kovacevic, N., Potts, D. & Vaughan, P. (2001) Progressive failure in clay embankments due to seasonal climate changes. *Proceedings of the The International Conference on Soil*

Mechanics and Geotechnical Engineering AA BALKEMA PUBLISHERS, 3, pp. 2127-2130.

Kovacevic, N., Higgins, K. G., Potts, D. M. & Vaughan, P. R. (2007) Undrained behaviour of brecciated upper lias clay at empingham dam. *Géotechnique*, **57** (2), 181-195.

Lees, A., MacDonald, G., Sheerman-Chase, A. & Schmidt, F. (2013) Seasonal slope movements in an old clay fill embankment dam. *Canadian Geotechnical Journal*, **50** (5), 503-520.

Leung, A. K., Garg, A., Coo, J. L., Ng, C. W. W & Hau, B. C. H (2015) Effects of the roots of Cynodon dactylon and Schefflera heptaphylla on water infiltration rate and soil hydraulic conductivity. *Hydrological Processes*, **29**, 3342-3354

Li, J. & Zhang, L. (2011) Study of desiccation crack initiation and development at ground surface. *Engineering Geology*, **123** (4), 347-358.

Löbmann, M.T., Geitner, C., Wellstein, C. Zerbe, S. (2020). The influence of herbaceous vegetation on slope stability–A review. Earth-Science Reviews, 209, p.103328.

Mao, Z., Bourrier, F., Stokes, A. & Fourcaud, T. (2014). Three-dimensional modelling of slope stability in heterogeneous montane forest ecosystems. Ecological Modelling, 273, pp.11-22.

Mualem, Y. (1976) A new model for predicting the hydraulic conductivity of unsaturated porous media. *Water resources*, **12** (3), 513-522

Network Rail (2022) NR/L2/TRK/001 Module 11 "Track geometry - inspections and minimum action"

Ng, C. W., Wang, B. & Tung, Y. (2001) Three-dimensional numerical investigations of groundwater responses in an unsaturated slope subjected to various rainfall patterns. *Canadian Geotechnical Journal*, **38** (5), 1049-1062

Ng, C.W., Zhang, Q., Ni, J. & Li, Z. (2021). A new three-dimensional theoretical model for analysing the stability of vegetated slopes with different root architectures and planting patterns. Computers and Geotechnics, 130, p.103912.

Ng, C.W.W., Zhang, Q., Zhou, C. & Ni, J. (2022). Eco-geotechnics for human sustainability. Science China Technological Sciences, 65(12), pp.2809-2845.

Ni, J. J., Leung, A. K. & Ng, C. W. W. (2019a) Modelling effects of root growth and decay on soil water retention and permeability. *Canadian Geotechnical Journal*, **56**, 1049-1055

Ni, J., Leung, A.K. & Ng, C.W. (2019b). Unsaturated hydraulic properties of vegetated soil under single and mixed planting conditions. Géotechnique, 69(6), pp.554-559.

Nyambayo, V., Potts, D. & Addenbrooke, T. (2004) The influence of permeability on the stability of embankments experiencing seasonal cyclic pore water pressure changes. *Proceedings of the Advances in Geotechnical Engineering. The Skempton Conference. Thomas Telford, London*. pp. 898-910.

Nyambayo, V. P. & Potts, D. M. (2010) Numerical simulation of evapotranspiration using a root water uptake model. *Computers and Geotechnics*, **37**, 175-186.

O'Brien, A. (2007) Rehabilitation of urban railway embankments: Investigation, analysis and stabilisation. In: *14th European Conference on Soils Mechanics and Geotechnical Engineering, 24-27 September 2007, Madrid, Spain*. pp. 125-143.

O'Brien, A. S., Ellis, E. A. & Russell, D. (2004) Old railway embankment clay fill: Laboratory experiments, numerical modelling and field behaviour. *Proceedings of the Advances in Geotechnical Engineering. The Skempton Conference. Thomas Telford, London*. pp. 911-921.

O'Brien, A. S. (2013) "*The assessment of old railway embankments: Time for a change?*" *Partial saturation in compacted soils: Geotechnique symposium in print 2011*, pp. 19-32.

Pedone, G., Tsiampousi, A., Cotecchia, F. & Zdravkovic, L. (2022) Coupled hydro-mechanical modelling of soil-vegetation-atmosphere interaction in natural clay slopes. *Canadian Geotechnical Journal*, **59** (2), 272-290

Potts, D.M., Kovacevic, N. and Vaughan, P.R., 2009. Delayed collapse of cut slopes in stiff clay. In Selected papers on geotechnical engineering by PR Vaughan (pp. 362-391). Thomas Telford Publishing.

Rouainia, M., Davies, O., O'Brien, T. & Glendinning, S. (2009) Numerical modelling of climate effects on slope stability. *Proceedings of the Proceedings of the Institution of Civil Engineers-Engineering Sustainability*. Thomas Telford Ltd, 162, pp. 81-89.

Russell, D., Ellis, E., O''BRIEN, A. & McGinnity, B. (2000) Role of vegetation in the stability and servicibility of railway embankments. *Proceedings of the PROCEEDINGS OF THE INTERNATIONAL CONFERENCE, RAILWAY ENGINEERING 2000, HELD LONDON, UK, JULY 2000-CD-ROM*.

Sitarenios, P, Casini, F., Askarinejad, A & Springman, S. (2021) Hydro-mechanical analysis of a superficial landslide triggered by artificial rainfall: the Ruedlingen field experiment. *Geotechnique*, **71** (2), 96-109

Smethurst, J., Clarke, D. & Powrie, W. (2012) Factors controlling the seasonal variation in soil water content and pore water pressures within a lightly vegetated clay slope. *Geotechnique*, **62** (5), 429.

Smethurst, J., Briggs, K. M., Powrie, W., Ridley, A. & Butcher, D. J. E. (2015) Mechancial and hydrological impacts of tree removal on a clay fill railway embankment. *Geotechnique*, **65** (11), 869-882.

Switala, B. M. & Wu, W. (2018) Numerical modelling of rainfall-induced instbility of vegetated slopes. Geotechnique, https://doi.org/10.1680/jgeot.16.P.176

Świtała, B.M., Wu, W. & Wang, S. (2019). Implementation of a coupled hydro-mechanical model for root-reinforced soils in finite element code. Computers and Geotechnics, 112, pp.197-203.

Taborda, D., Potts, D. & Zdravkovic, L. (2016) On the assessment of energy dissipated through hysteresis in finite element analysis. *Computers and Geotechnics*, **71**, 180-194.

Taborda, D. M. G., Kontoe, S. & Tsiampousi, A. (2023a) “IC MAGE Model 01 – strain-hardening/softening Mohr-Coulomb failure criterion with isotropic small strain stiffness (Version 2.0)”. Zenodo. doi: 10.5281/zenodo.7565062

Taborda, D. M. G., Kontoe, S. & Tsiampousi, A. (2023b) "IC MAGE UMIP – universal model interface for PLAXIS (Version 3.3)". Zenodo. doi: 10.5281/zenodo.7564989

Tsaparas, I., Rahardjo, H., Toll, D. G. & Leong, E. C. (2002) Controlling parameters for rainfall-induced landslides. *Computers and Geotechnics*, **29** (1), 1-27.

Tsiampousi, A., Zdravković, L. & Potts, D.M. (2013a). A new Hvorslev surface for critical state type unsaturated and saturated constitutive models. Computers and Geotechnics, 48, pp.156-166.

Tsiampousi, A., Zdravkovic, L. & Potts, D. M. (2013b) Variation with time of the factor of safety of slopes excavated in unsaturated soils. *Computers and Geotechnics*, **48**, 167-178.

Tsiampousi, A., Vitsios, I., Zdravkovic, L. & Potts, D. (2014) Effect of previous stress history and vegetation on the coefficient of earth pressure at-rest, k0, in London clay. *Numerical Methods in Geotechnical Engineering*, 209-214.

Tsiampousi, A., Zdravkovic, L. & Potts, D. (2016) Soil-atmosphere interaction in unsaturated cut slopes. *N In: Delage P, Ghabezloo S, Tang A-M, Cui Y-J, Pereira J-M (eds) Proceedings of 3rd European conference on unsaturated soils. EDP Sciences, Paris*. E3S Web of Conferences 9, 08004 (2016)

Tsiampousi, A., Zdravkovic, L. & Potts, D. (2017) Numerical study of the effects of soil-atmosphere interaction on the stability and serviceability of cut slopes in London clay. *Canadian Geotechnical Journal*, **54**, 405-418

Tsiampousi, A. (2023a) 3D effects of soil-atmosphere interaction on infrastructure slope stability. *Proceedings 8th International Conference on Unsaturated Soils* (accepted for publication)

Tsiampousi, A., (2023b). The importance of permeability in modelling soil-atmosphere interaction. In E3S Web of Conferences (Vol. 382, p. 06010). EDP Sciences.

van Genuchten, M. T. (1980) A closed-form equation for predicting the hydraulic conductivity of unsaturated soils. Soil Science Society of America Journal, **44** (5), 892-898

Wu, T.H. (2013). Root reinforcement of soil: review of analytical models, test results, and applications to design. Canadian Geotechnical Journal, 50(3), pp.259-274.

Yildiz, A., Graf, F., Rickli, C. & Springman, S. M. (2018) Determination of the shearing behaviour of root-permeated soils with a large-scale direct shear apparatus. CATENA, **16**, 98-113

Tables

Table 1: Model parameters for weathered and unweathered London clay

Strength parameters		
Angle of shearing resistance, φ' (degrees)	**Cohesion, c' (kPa)**	**Angle of dilation, υ (degrees)**
23°	7.0	0.0

Small strain stiffness parameters											
G_0 **(kPa)**	K_0 **(kPa)**	G_{min} **(kPa)**	K_{min} **(kPa)**	m_G **( )**	m_k **( )**	a_0 **( )**	b **( )**	$R_{G,min}$ **( )**	$R_{k,min}$ **( )**	r_0 **( )**	s **( )**
955	1665	2000	3000	0.7	0.7	1.81E-4	1.3	5E-2	7.9E-2	3E-4	1.1

Table 2: Hydraulic parameters for weathered London clay

k_{sat} **(m/s)**	S_{sat} **( )**	S_{res} **(kPa)**	g_n **( )**	g_a **(1/m)**	g_l **( )**
4.3E-8	1	0	1.5	0.15	0